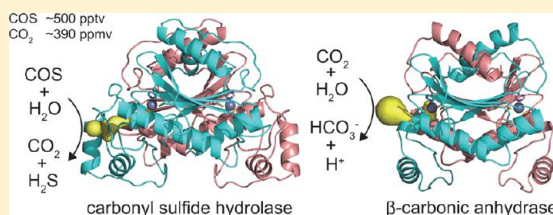


Carbonyl Sulfide Hydrolase from *Thiobacillus thioparus* Strain THI115 Is One of the β -Carbonic Anhydrase Family EnzymesTakahiro Ogawa,^{†,⊗} Keiichi Noguchi,[‡] Masahiko Saito,^{†,▽} Yoshiko Nagahata,^{§,○} Hiromi Kato,^{†,▲} Akashi Ohtaki,^{||,¶} Hiroshi Nakayama,[⊥] Naoshi Dohmae,[⊥] Yasuhiko Matsushita,[#] Masafumi Odaka,^{||} Masafumi Yohda,^{||} Hiroshi Nyunoya,[#] and Yoko Katayama^{*,†,§}[†]Department of Science of Resources and Environment, United Graduate School of Agricultural Science, [§]Department of Environmental Science on Biosphere, Graduate School of Agriculture, and [#]Gene Research Center, Tokyo University of Agriculture and Technology, Fuchu, Tokyo 183-8509, Japan[‡]Instrumentation Analysis Center and ^{||}Department of Biotechnology and Life Science, Graduate School of Technology, Tokyo University of Agriculture and Technology, Koganei, Tokyo 184-8588, Japan[⊥]Biomolecular Characterization Team, Advanced Technology Support Division, Advanced Science Institute, RIKEN, Wako, Saitama 351-0198, Japan

S Supporting Information

ABSTRACT: Carbonyl sulfide (COS) is an atmospheric trace gas leading to sulfate aerosol formation, thereby participating in the global radiation balance and ozone chemistry, but its biological sinks are not well understood. *Thiobacillus thioparus* strain THI115 can grow on thiocyanate (SCN^-) as its sole energy source. Previously, we showed that SCN^- is first converted to COS by thiocyanate hydrolase in *T. thioparus* strain THI115. In the present work, we purified, characterized, and determined the crystal structure of carbonyl sulfide hydrolase (COSase), which is responsible for the degradation of COS to H_2S and CO_2 , the second step of SCN^- assimilation. COSase is a homotetramer composed of a 23.4 kDa subunit containing a zinc ion in its catalytic site. The amino acid sequence of COSase is homologous to the β -class carbonic anhydrases (β -CAs). Although the crystal structure including the catalytic site resembles those of the β -CAs, CO_2 hydration activity of COSase is negligible compared to those of the β -CAs. The $\alpha 5$ helix and the extra loop (Gly150–Pro158) near the N-terminus of the $\alpha 6$ helix narrow the substrate pathway, which could be responsible for the substrate specificity. The $k_{\text{cat}}/K_{\text{m}}$ value, $9.6 \times 10^5 \text{ s}^{-1} \text{ M}^{-1}$, is comparable to those of the β -CAs. COSase hydrolyzes COS over a wide concentration range, including the ambient level, *in vitro* and *in vivo*. COSase and its structurally related enzymes are distributed in the clade D in the phylogenetic tree of β -CAs, suggesting that COSase and its related enzymes are one of the catalysts responsible for the global sink of COS.



■ INTRODUCTION

Carbonyl sulfide (COS; $\text{O}=\text{C}=\text{S}$) is the most abundant sulfur compound in the troposphere,^{1,2} with the average mixing ratio of ~ 500 parts per trillion by volume (pptv)¹ and is an important source of stratospheric sulfate aerosol influencing the Earth's radiation balance^{3–5} and ozone chemistry.⁶ COS is also regarded as a greenhouse gas due to its high global-warming potential.⁷ Although there is still uncertainty in the global budget of atmospheric COS, both anthropogenic and natural activities have strong influences on the processes of source and sink of COS.^{8,9} Biological COS degradation in a soil environment is considered an important COS sink, as the uptake of COS was inhibited by the addition of ethoxzolamide, an inhibitor for carbonic anhydrase (CA; EC 4.2.1.1),¹⁰ and by autoclaving the soil.¹¹ Therefore, studying COS degrading enzymes in the soil is important for solving global environmental problems.

CA, a ubiquitous enzyme involving numerous biological processes, and three other enzymes have been demonstrated to

catalyze the transformation of COS (Table 1).^{12–22} These enzymes are diversely distributed, but their activities on COS are much less efficient than their activities on their natural substrates. Rather, COS has been used as an inhibitor of these enzymes. Recently, carbon disulfide (CS_2) hydrolase from an acidophilic and thermophilic archaeon, *Acidianus* sp. strain A1-3, has been shown to efficiently catalyze the hydrolysis of COS as well as CS_2 .²³ However, its habitat is limited in the extreme environments such as solfataric springs.²⁴ There have been no reports on an enzyme that is found commonly and that only catalyzes the degradation of COS. Furthermore, the understanding of COS degradation at the enzyme level is critical to elucidate soil microorganisms as a major sink of COS.⁹

Thiobacillus thioparus is an obligately chemolithoautotrophic and mesophilic sulfur-oxidizing bacterium. It is widely distributed in soil and freshwater.²⁵ *T. thioparus* strain

Received: August 4, 2012

Published: February 13, 2013

Table 1. Comparison of Enzyme Kinetics of COS Degradation between COSase and Enzymes Harboring COS Degrading Activity

enzyme	organism	k_{cat} (s^{-1})	K_{m} (μM)	$k_{\text{cat}}/K_{\text{m}}$ ($\text{s}^{-1} \text{M}^{-1}$)	reference
COSase	<i>T. thioparus</i> strain THI115	58 ^a	60	9.6×10^5 ^a	this study
CS ₂ hydrolase	<i>Acidianus</i> sp. strain A1–3	1800	22	8.2×10^7 ^b	23
CA	<i>Bos taurus</i>	41	1.9×10^3	2.2×10^4	17
nitrogenase	<i>Azotobacter vinelandii</i>	0.16	3.1×10^3	52 ^b	20
CO dehydrogenase	<i>Rhodospirillum rubrum</i> ATCC11170 ^T	0.52	2.2	2.4×10^5 ^b	21
RuBisCO	<i>Rhodospirillum rubrum</i>	6.3	5.6×10^3	1.1×10^3	22
RuBisCO	<i>Spinacia oleracea</i>	3.8	1.8×10^3	2.2×10^3	22

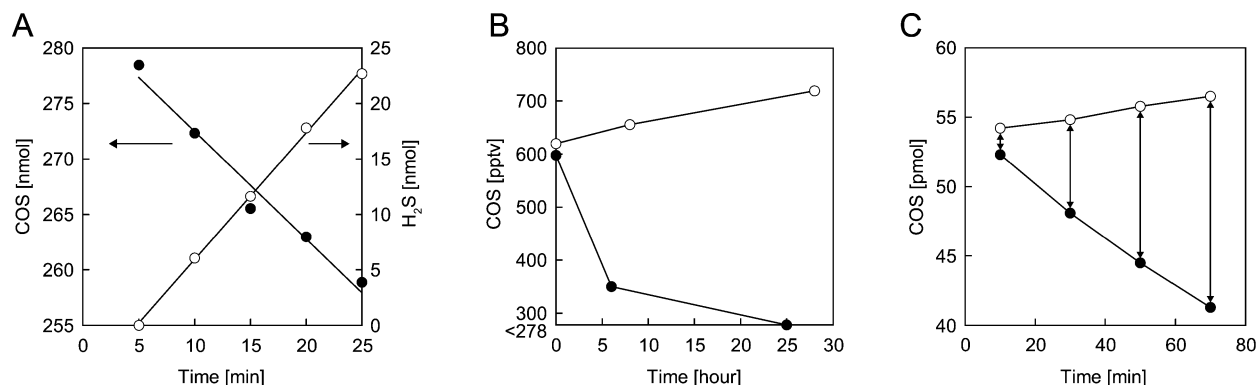
^aCalculated by dimer. ^bCalculated based on reference.

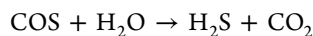
Figure 1. Degradation of COS by whole cells and COSase. (A) Time course of COS (●) degradation and H₂S (○) production by COSase. COSase (0.066 μg) was injected into a vial (4.9 mL) filled with 320 nmol of COS and 20 nmol of H₂S. Because addition of the enzyme solution into the vial caused disturbance of COS and H₂S concentrations, the sampling of the headspace gas was started 5 min after the addition of the enzyme. (B) Degradation of ambient level COS by whole cells. Symbols: ●, with cells; ○, without cell. Cells in a 10 mL culture containing fully grown *T. thioparus* strain THI115 were put in a Petri dish and then placed in a gas-sampling bag (~3 L). (C) Degradation of ambient level of COS by recombinant COSase. Symbols: ●, with COSase; ○, without COSase. The reaction was started by adding the reaction mixture containing 10 μg of COSase to a gas-sampling bag as described in the text. The volume of the introduced nitrogen gas that contained 510 pptv (55 pmol) of COS was 2.7 L. The amounts of COS hydrolyzed by COSase was calculated as the difference between the concentrations with and without COSase (indicated by arrows).

THI115 was isolated as a thiocyanate (SCN^-)-degrading microorganism from activated sludge used for the wastewater treatment of a coke-oven factory.²⁶ SCN^- is common in nature and is generated by the hydrolysis of glucosinolates in plants and the detoxication of cyanide in mammals.^{27,28} In addition to its natural origins, various industrial processes including coal gasification have been considered part of its anthropogenic origin.²⁸ Enzymatic transformation of SCN^- is initiated by thiocyanate hydrolase (SCNase; EC 3.5.5.8), which was first identified in *T. thioparus* strain THI115.²⁶ SCNase is a non-corrin cobalt enzyme that is highly similar to nitrile hydratases^{29–31} and hydrolyzes SCN^- to ammonia and COS.²⁶ The resultant COS is metabolized to hydrogen sulfide (H₂S), which is further oxidized to sulfate as the end product to produce energy.³² Thus, COS hydrolysis in *T. thioparus* strain THI115 must be linked to a metabolic pathway of chemolithotrophic energy formation. However, the enzyme responsible for the conversion of COS remains unknown.

In this study, we describe the purification, gene cloning, characterization, and crystallography of the novel enzyme carbonyl sulfide hydrolase (COSase) from *T. thioparus* strain THI115. COSase acts over a wide concentration range, including the ambient level, highlighting the possibility that COSase is one of the mediators that act as a COS sink.

RESULTS

Purification and Characterization of COSase. A crude extract of *T. thioparus* strain THI115 initially degraded 1200 ppmv of COS at a rate of $0.085 \mu\text{mol mg}^{-1} \text{min}^{-1}$, indicating that the bacterium possesses an enzyme catalyzing the degradation of COS. This enzyme was purified by sequential column chromatography and ran as a single band on sodium dodecyl sulfate–polyacrylamide gel electrophoresis with a subunit molecular mass of 27 kDa (Figure S1A). Inductively coupled plasma mass spectrometric analysis revealed that the enzyme contained one zinc ion per subunit. The N-terminal 35 amino acid sequence was determined to be MEKSNTDAL-LENNRLYAGGQATHRPGHPGMQPIQP. The decrease of COS by enzymatic degradation, balanced with the production of H₂S throughout the incubation (Figure 1A), indicated that the overall reaction by the enzyme was as follows:



We named the enzyme carbonyl sulfide hydrolase (COSase).

Gene Cloning and Expression of COSase in *Escherichia coli*. Using an oligo-DNA probe designed for the N-terminal amino acid sequence, 1864 bp, including 660 bp of open reading frame encoding the COSase gene, was identified (Figure S2A). Southern blotting analysis using the COSase gene as a probe detected one band for the *T. thioparus* strain THI115 genomic DNA digested with each restriction enzyme. This result confirmed the presence of only one copy of the

COSase gene in the genome (Figure S3). COSase shares a high amino acid sequence homology with β -CAs and retains most of their highly conserved residues, including the Zn-binding site (Figure S2B). COSase was expressed in *E. coli*, and the molecular mass of the purified COSase was determined to be ~ 94 kDa by size-exclusion chromatography with multi-angle light scattering (SEC-MALS), suggesting it has a homotetrameric structure (Figure S1B).

Activity of Recombinant COSase on COS, CO₂, and CS₂. The COSase expressed in *E. coli* exhibited a hydrolysis activity of $18 \mu\text{mol mg}^{-1} \text{min}^{-1}$ for COS at a COS concentration of $26 \mu\text{M}$ (1400 ppmv), approximately equivalent to that of the enzyme purified from *T. thioparus* strain TH115. COSase activity followed Michaelis–Menten-type kinetics with $K_m = 60 \mu\text{M}$ for COS and $k_{\text{cat}} = 58 \text{ s}^{-1}$. COSase exhibited the CO₂ hydration activity with a rate of $24 \mu\text{mol mg}^{-1} \text{min}^{-1}$, which corresponds to a turnover number (TON) of 19 s^{-1} by dimer at a CO₂ concentration of 17 mM . Although COSase shares a high similarity with β -CAs, its CO₂ hydration activity was ~ 3 – 4 orders of magnitude smaller than those of β -CAs.³³ Furthermore, we examined COSase's CS₂ hydrolysis activity and found that at a CS₂ concentration of $460 \mu\text{M}$, H₂S was produced at a rate of $3.9 \mu\text{mol mg}^{-1} \text{min}^{-1}$ with a trace amount of COS ($<0.1 \mu\text{mol mg}^{-1} \text{min}^{-1}$). The CS₂ hydrolysis activity of COSase is much smaller than that of the *Acidianus* sp. strain A1-3 CS₂ hydrolase ($\sim 30 \mu\text{mol mg}^{-1} \text{min}^{-1}$).²³

Crystal Structure of COSase. To understand the substrate specificity, the crystal structures of COSase in its native and SCN[−]-complexed forms were determined at 1.20 and 1.33 Å resolution, respectively. SCN[−] was used as a COS analogue because of its similar size and shape. The structure of the native COSase can be superimposed to the structure of the SCN[−]-complex with a root-mean-squared deviation (RMSD) of 0.16 Å for 213 C α pairs and 0.38 Å for all atoms. Hereafter, we describe the structure of COSase complexed with SCN[−]. A COSase subunit consists of a five-stranded β -sheet core ($\beta 1$ – $\beta 5$) and four flanking α -helices ($\alpha 1$, $\alpha 2$, $\alpha 3$, and $\alpha 6$), with two additional helices ($\alpha 4$ and $\alpha 5$) protruding from its core. Pairs of the subunits assemble into tightly packed homodimers to form an extended ten-stranded β -sheet across the dimer (Figure 2A). Similar dimeric structures were commonly found in the crystal structures of β -CAs.³⁴ Two symmetrically related dimers are weakly associated to form homotetramers. The tetramerization interface of $\sim 960 \text{ Å}^2$ /subunit is smaller than the dimerization interface ($\sim 3420 \text{ Å}^2$ /subunit). Consistent with the SEC-MALS results, the homotetramer found in the crystal is likely to be the biologically active structure in solution.

Structure around the Catalytic Site in SCN[−]-Complexed COSase. The catalytic site is located at the interface between the two subunits of the homodimer and largely sequestered from solvent. As predicted by sequence conservation, a zinc ion coordinates residues Cys44, His97, and Cys100 from the same subunit with coordination distances of 2.28 Å (Zn–S γ (Cys44)), 2.04 Å (Zn–N ϵ (His97)), and 2.31 Å (Zn–S γ (Cys100)), respectively (Figure 2B). The fourth site is occupied by a water molecule with a coordination distance of 2.08 Å. The water molecule is stabilized by hydrogen bonding to the carboxylate group of neighboring Asp46 (2.59 Å), which formed the salt bridge with Arg48, and the amide nitrogen of Gly101 (2.98 Å). These interactions in the catalytic site of COSase are essentially identical to those found in β -CAs.³⁴ An

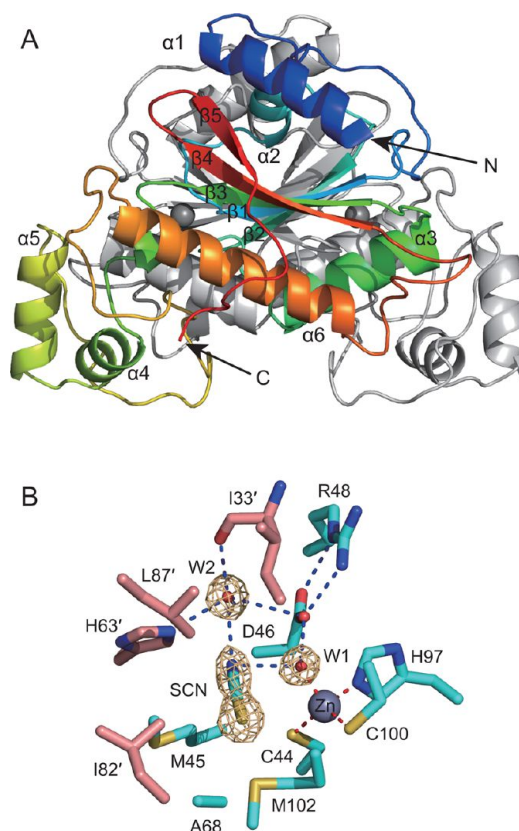


Figure 2. Crystal structure of COSase. (A) The ribbon diagram of the dimer structure. One subunit is colored blue to red from the N to the C terminus, and the other one is shown in gray. The zinc ions in the catalytic site are indicated as dark gray spheres. (B) The catalytic site of COSase complex with SCN[−]. The residues originating from one subunit are shown in cyan and those from the other in pink. The OMIT electron density map (5σ) for the SCN[−] and surrounding water molecules are colored orange. The zinc ion (dark gray sphere) is coordinated by two cysteine and one histidine residues and a water molecule (red sphere). Interactions between the zinc ion and its ligands are shown as red broken lines. Blue broken lines indicate the hydrogen bonds. Nitrogen, oxygen, and sulfur atoms are shown in blue, red, and yellow, respectively.

SCN[−] molecule is located in the catalytic-site pocket and interacts with a zinc-bound water molecule (O(W1)···N(SCN) = 3.00 Å), a water molecule hydrogen-bonded to His63' (meaning His63 of the other subunit in the homodimer, O(W2)···N(SCN) = 3.01 Å). In addition, the SCN[−] molecule is surrounded by the Cys44, Met45, Asp46, Ala68, Met102, Ile33', His63', Leu67', and Ile82' residues (Table S1). Since the catalytic-site pocket of COSase is small and hydrophobic, its shape is perfectly matched with that of a SCN[−] molecule.

Structural Comparison with β -CAs. Crystal structures of β -CAs can be categorized into two subclasses, the plant-type and Cab-type classes, depending on the conserved residues near their active-site pockets.³⁵ The residues Gln, Phe, and Tyr are conserved in the plant-type β -CAs, but variable in the Cab type. The corresponding residues in COSase are Ile33, His63, and Ile82, respectively, suggesting that COSase resides in the Cab type. Structural searches with the program DALI³⁶ revealed that COSase has a high similarity to the *Mycobacterium tuberculosis* β -CA Rv1284 (Protein Data Bank (PDB) code 1YLK)³⁷ and the *Methanobacterium thermoautotrophicum* β -CA (PDB code 1G5C)³⁸ with RMSD values of 1.2 and 2.4 Å for 146 C α pairs,

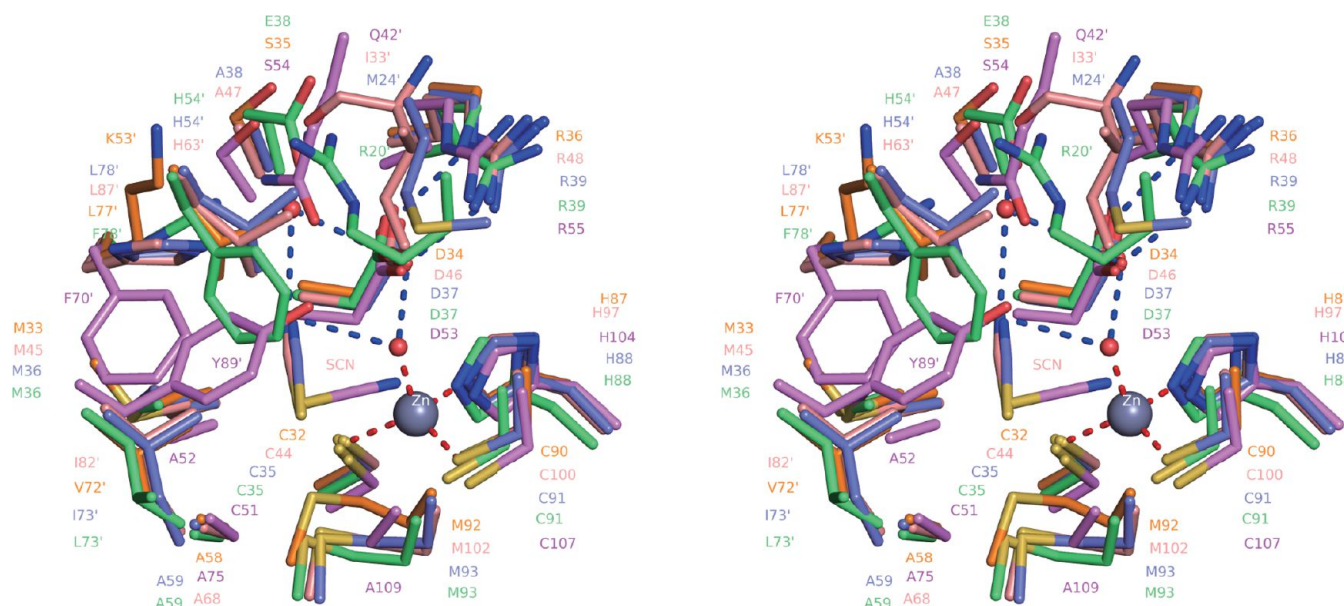


Figure 3. Overlay of the catalytic sites of COSase (pink), the *Myc. tuberculosis* β -CA Rv1284 (blue), the *Myc. tuberculosis* β -CA Rv3588c (purple), the *Meth. thermoautotrophicum* β -CA (orange) and the *Acidianus* sp. strain A1–3 CS_2 hydrolase (green). The zinc ion and water molecules in COSase are represented as gray and red spheres, respectively. Interactions between the zinc ion and its ligands are shown as red broken lines. Blue broken lines indicate the hydrogen bonds. Nitrogen, oxygen, and sulfur atoms are shown in blue, red, and yellow, respectively.

respectively. Since both β -CAs can be classified into Cab type, COSase appears more closely related to the Cab type than to the plant type. The notable structural differences from the Cab-type β -CAs are observed in the $\beta 3$ – $\beta 4$ connection, especially in the $\alpha 5$ helix and the following loop (Gly129–Ala135). This arrangement of the $\alpha 5$ helix in the overall architecture has never been observed in the structures of β -CAs and may be unique to COSase. In addition, COSase has an extra loop (Gly150–Pro158) near the N-terminus of the $\alpha 6$ helix. All of these additional structures found in COSase are located near its active-site pocket. As shown in the structure-based alignment (Figure S2B), the COSase sequence has an insertion in this region relative to the β -CAs.

The catalytic site of COSase is analogous to those of the *Myc. tuberculosis* β -CA Rv1284³⁷ and the *Meth. thermoautotrophicum* β -CA³⁸ (Figure 3). An SCN^- molecule from the buffer solution is located in the catalytic-site pocket of *Myc. tuberculosis* β -CA Rv1284, and its position is almost the same as that in COSase. On the other hand, an SCN^- molecule directly coordinates the zinc ion in the tetrameric form of *Myc. tuberculosis* β -CA Rv3588c which can be categorized into plant type.³⁹ The recent structural study on the CS_2 hydrolase from the *Acidianus* sp. strain A1-3 has revealed that the enzyme has the β -CA-type fold and catalytic-site structure.²³ The catalytic sites of COSase and the CS_2 hydrolase are similar to each other, and the notable differences are observed in the Ala47, Ile33', and Leu87', which are substituted with Glu38, Arg20', and Phe78' in the CS_2 hydrolase, respectively (Figure 3). These results suggest that COSase, Cab-type β -CA, and CS_2 hydrolase have similar catalytic mechanisms in spite of their different substrate specificity.

Inhibition of COSase Activity by SCN^- . The structure of SCN^- -complexed COSase implied that this molecule may inhibit COS hydration activity. Because CA is inhibited by various anion including SCN^- ,⁴⁰ we examined the effect by adding 10 and 100 mM NaSCN to reaction mixture at 18 μM of COS. The residual activities in the presence of 10 and 100

mM NaSCN were 70% and 20%, respectively, showing that SCN^- acts as a very weak inhibitor against COSase.

COS Hydrolysis Activity at Ambient Level. Considering the effect of COSase on the atmosphere, we examined the degradation of ambient level COS by whole cells of *T. thioparus* strain THI115 (Figure 1B). Initially, 600 pptv COS decreased to 350 pptv in 6 h and then gradually reached less than the detection limit (280 pptv) in 25 h. A small increase of COS in the control appeared to originate from the mTC medium because no COS production was detected in the absence of the medium. The purified COSase retained its COS hydrolysis activity of 22 $\text{pmol mg}^{-1} \text{min}^{-1}$, even under the ambient mixing ratio (Figure 1C). These results suggest that COSase from *T. thioparus* strain THI115 functions as one of the microbial sinks for ambient COS.

DISCUSSION

The conservation in amino acid sequence and crystal structure between COSase and β -CAs indicates that COSase belongs to the β -CA super family. However, COSase is unique in its substrate specificity. It shows high COS degradation activity but has little CO_2 hydration activity and poor CS_2 hydrolysis activity compared to β -CAs and CS_2 hydrolase, respectively.^{23,33} Unfortunately, we could not determine the kinetic parameters of COSase for CO_2 hydration because of its low reactivity. But, the fact that the COS hydrolysis activity at a COS concentration of 26 μM is comparable to the CO_2 hydration activity at a CO_2 concentration of 17 mM indicates that COSase is at least moderately specific for COS compared to CO_2 .³³ Additionally, COSase is very weakly inhibited by SCN^- , one of the inhibitors known against CA.^{18,19,40} *T. thioparus* strain THI115 can use SCN^- as its sole energy source. Previously, we demonstrated SCNase catalyzes the first step of SCN^- degradation to generate energy for the growth. The COS hydrolyzing activity in the crude *T. thioparus* strain THI115 extract reaches $\sim 0.4\%$ of that of the purified COSase. The $k_{\text{cat}}/K_{\text{m}}$ value of COSase for COS is much larger than that of

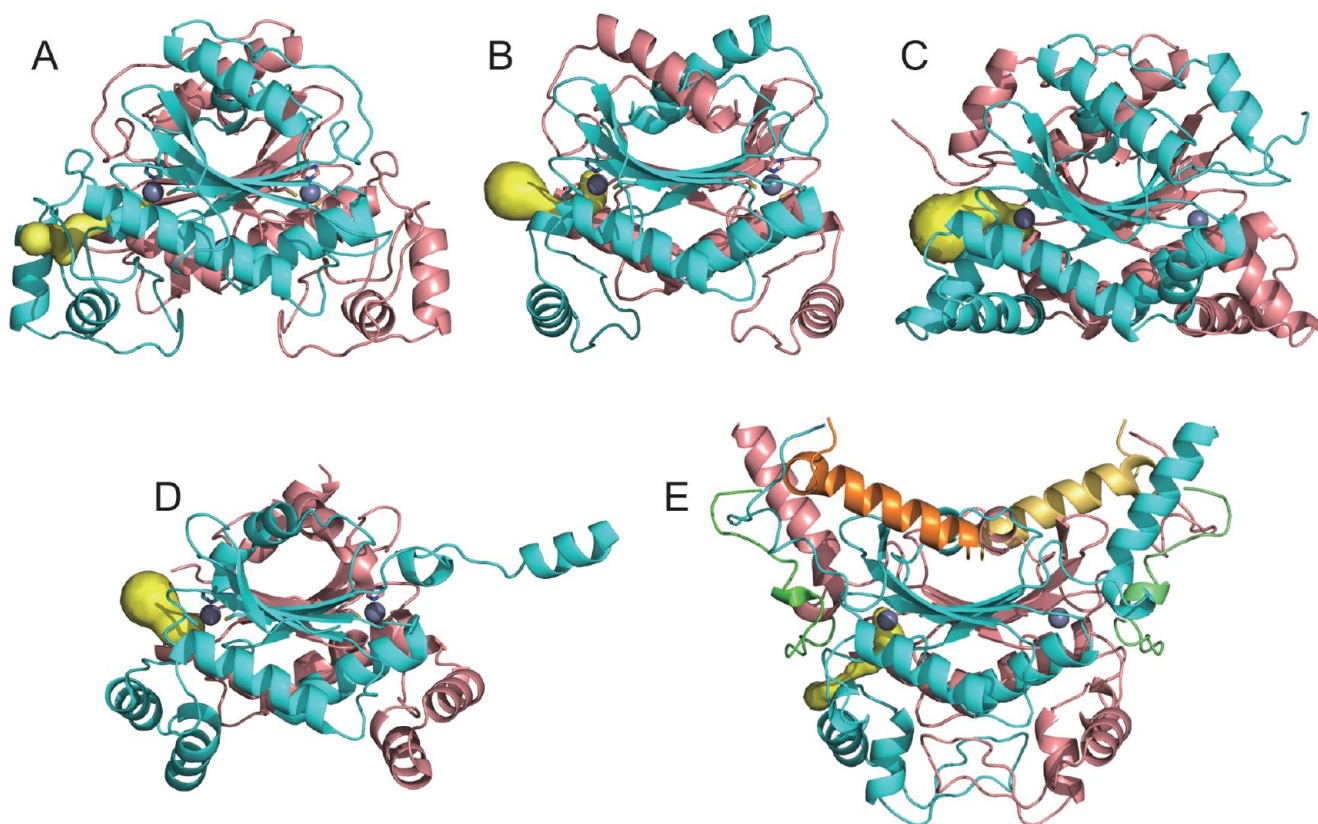


Figure 4. Possible substrate tunnels (yellow) from the active site to the surrounding solvent calculated using CAVER: (A) COSase, (B) *Myc. tuberculosis* β -CA Rv1284, (C) *Myc. tuberculosis* β -CA Rv3588c (tetrameric form), (D) *Meth. thermoautotrophicum* β -CA, and (E) CS_2 hydrolase from the *Acidianus* sp. strain A1-3. One subunit is shown in cyan and the other in pink. Dark orange and dark green parts in (E) correspond to the N- and C-terminals of the adjacent subunit, and light orange and light green parts represent those of the opposite subunit. Dark gray spheres represent the zinc ions in the active sites.

SCNase for SCN^- , and the large $k_{\text{cat}}/K_{\text{m}}$ value of COSase is appropriate for the hydrolysis of the COS produced by SCNase in *T. thioparus* strain TH115.²⁶ Thus, COSase is competent for the second step of SCN^- degradation in *T. thioparus* strain TH115. Additionally, COSase is a novel β -CA family enzyme that uses COS as a natural substrate.

The conservation of the environment around the catalytic zinc center and the hydroxide ligand suggests that the catalytic mechanism of COSase for COS is conserved with that proposed for β -CAs and CS_2 hydrolase.^{23,34} Briefly, the hydroxide ion coordinated to the zinc ion nucleophilically attacks the carbon atom of the COS molecule to generate the intermediate having the zinc ion bound both to the hydroxide oxygen and by the sulfur atom of the COS molecule. The subsequent release of the oxygen from the zinc ion results in the formation of the product, CO_2 . Then, a solvent water molecule reacted with the sulfur-coordinated zinc ion, resulting in the regeneration of the active site and release of H_2S (Figure S4). The reason for the substrate specificity of COSase is not well understood because the structure around the catalytic site of COSase is highly conserved with those of the Cab-type β -CAs from *Myc. tuberculosis*³⁷ and *Meth. thermoautotrophicum*³⁸ (Figure 3) and because both β -CAs hydrate CO_2 efficiently.^{41,42} We hypothesize that the difference in the CO_2 specificity between COSase and Cab-type β -CAs may be attributed to the accessibility of the CO_2 to the active site. Figure 4 shows the proposed substrate tunnels of COSase, the β -CAs from *Myc. tuberculosis* and *Meth. thermoautotrophicum*, and the CS_2 hydrolase from the *Acidianus* sp. strain A1-3 calculated using

CAVER.⁴³ These β -CAs have widely opened tunnels toward their surfaces, suggesting a diffusion-controlled catalytic mechanism. In contrast, the substrate pathway of COSase is highly hydrophobic and extremely narrow because of the $\alpha 5$ helix and the extra loop (Gly150–Pro158) near the N-terminus of the $\alpha 6$ helix. The size of the substrate pathway of COSase is wide enough for the uptake and release of COS and its products, H_2S and CO_2 , but would be too narrow for the release of the CO_2 -hydration product HCO_3^- . The *Acidianus* sp. strain A1-3 CS_2 hydrolase shows no CA activity despite its highly conserved catalytic site with β -CA structures.²³ Although the oligomeric states of COSase (tetramer) and the CS_2 hydrolase (hexadecamer) are different, their dimeric structures (Figure 4) and catalytic sites (Figure 3) are similar to each other. In the case of the CS_2 hydrolase, the N-terminal α -helix of the neighboring subunit in the dimer and the C-terminal loop from adjacent dimers in the hexadecamer were located near its catalytic-site pocket. Smeulders et al. have suggested that its substrate pathway is also hydrophobic and narrowed by its subunit interfaces among its hexadecameric structure.²³ Although the substrate pathways are restricted by different means, the structure around the substrate pathways could be responsible for the substrate specificity of both enzymes. However, we cannot rule out the possibilities of flexibility of the substrate pathway and other mechanisms controlling the substrate specificity because the pathway of some plant-type CAs are narrow but the activity is efficient.^{34,35} CS_2 hydrolysis activity of COSase is 7.7 times less than that of the *Acidianus* sp. strain A1-3 CS_2 hydrolase at a CS_2 concentration of 460 μM .

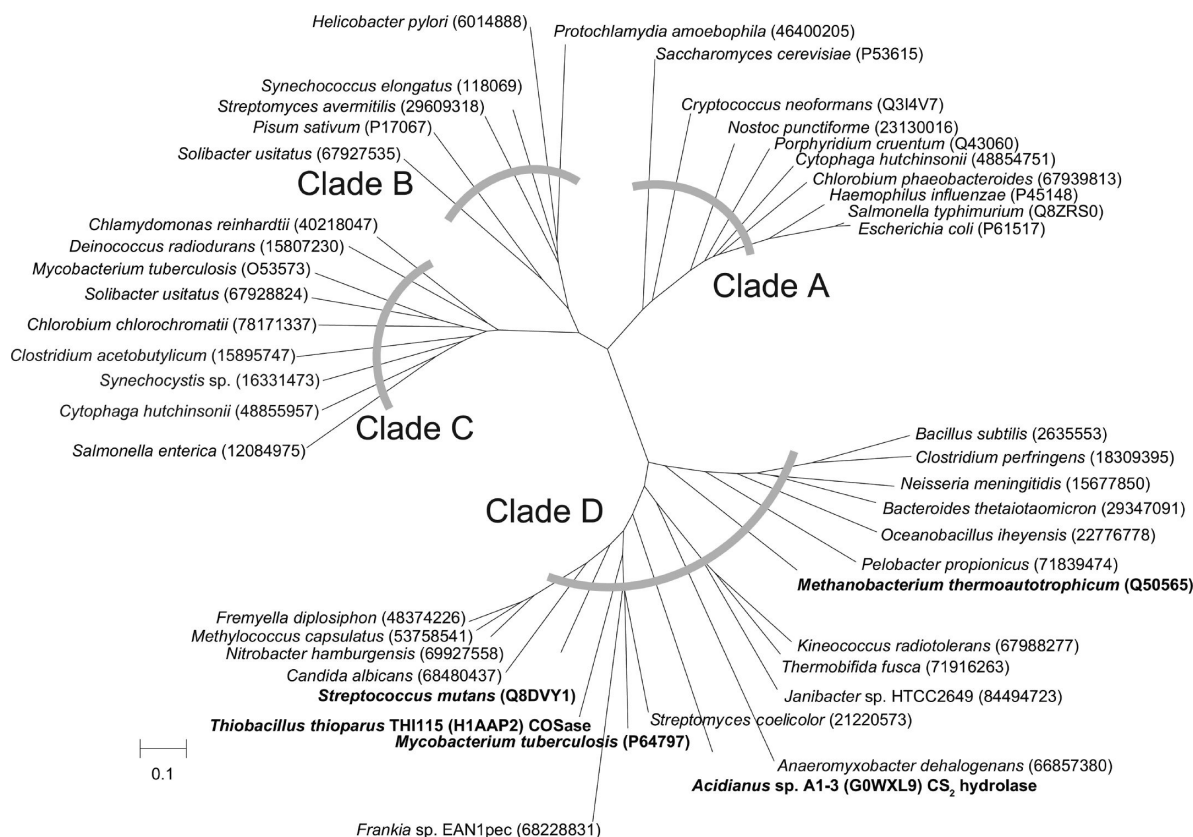


Figure 5. Phylogenetic tree of COSase and β -CAs. A phylogenetic tree was constructed with MEGA5⁶⁰ using sequences of COSase and β -CAs. β -CAs were selected from the PDB and used the sequences from UniProt Knowledgebase (UniProtKB) corresponding to β -CAs. β -CAs from the NCBI conserved domain database (CDD) were used to classify β -CAs into four clades. For each clade, single sequence data from eukarya and archaea, and those of bacteria that represent clades A, B, and C at the phylum level and clade D at the genus level were used to construct the tree when the sequence data of β -CAs was unavailable in PDB. Sequence data of *Halothiobacillus neapolitanus* deposited in PDB were not included due to the low homology with COSase. The transit peptide sequence of β -CA from *Pisum sativum* was also not included. The accession numbers of the β -CAs used here are indicated by its NCBI GI number or UniProtKB number and appear in parentheses. The COSase, CS₂ hydrolase, and β -CAs of clade D that were deposited to PDB are shown in bold.

The reason for this difference is not known. We note that Ile33 and Ala47 of COSase are substituted by Arg20 and Glu38 in CS₂ hydrolase (Figure 3). These residues increase the hydrophilicity of the corresponding area in the substrate pocket of CS₂ hydrolase and may affect its substrate specificity. Detailed studies on the substrate recognition mechanism of COSase are the subject for further investigations.

Both the K_m and k_{cat} of COSase for COS hydrolysis are ~ 2 orders of magnitude smaller than those of β -CAs for CO₂ hydration.^{41,42} As a result, the overall catalytic efficiency of COSase, $k_{cat}/K_m = 9.6 \times 10^5 \text{ s}^{-1} \text{ M}^{-1}$, is comparable to those of β -CAs. COSase shows the highest k_{cat}/K_m value among widely distributed enzymes with COS-degrading activity (Table 1). Previously, we showed that phylogenetically diverse soil bacteria belonging to Actinomycete, such as the genus *Mycobacterium* and the genus *Williamsia*, and to Proteobacteria, such as the genus *Cupriavidus*, exhibited COS-degrading activity.⁴⁴ Prokaryotic β -CAs are classified into four subgroups of clade: A, B, C, and D (Figure 5).^{33,45} Both the *T. thioparus* strain THI115 COSase and the *Acidianus* sp. strain A1-3 CS₂ hydrolase as well as two structurally similar β -CAs from *Myc. tuberculosis* and *Meth. thermoautotrophicum* belong to the clade D. We showed that soil bacteria in the genus *Mycobacterium* and filamentous fungus in the genus *Fusarium* degraded COS at an ambient mixing ratio.^{44,46} The enzymes with higher specificities for COS than CO₂, such as COSase, might be

widely distributed in clade D. β -CA is suggested to be an ancient enzyme.⁴⁵ Sulfur isotope analysis indicates that the mixing ratio of COS in the present troposphere is 10,000-times lower than that of the Archean eon more than 3 billion years ago.⁴⁷ Thus, it is important for COSase and/or COSase-related enzymes to harbor a higher specificity and catalytic efficiency to be a global sink of tropospheric COS in the present day. In addition, COSase contributes to biological energy production by a SCN[−] degradation pathway and is one of sulfur's biogeochemical processes.

CONCLUSIONS

In summary, COSase, a novel enzyme hydrolyzing COS to H₂S and CO₂, has been purified from *T. thioparus* strain THI115, a chemolithoautotrophic bacterium degrading SCN[−] to COS in its energy producing metabolism, and characterized structurally as well as biochemically. COSase exists as a homotetramer in which two pairs of subunits formed tightly associated dimers. Each subunit possesses a zinc ion in the active site. Although COSase shares high amino acid sequence homology and conserves structure including the zinc catalytic center as found in the β -CAs, CA activity is negligible compared to those of β -CAs. The difference in the substrate specificity could be due to the accessibility and hydrophobicity of the substrate pathway from the surface of molecule to the active site. COSase had K_m

= 60 μM for COS, $V_{\text{max}} = 74 \mu\text{mol mg}^{-1} \text{min}^{-1}$, and $k_{\text{cat}}/K_{\text{m}} = 9.6 \times 10^5 \text{ s}^{-1} \text{ M}^{-1}$, showing that COSase is one of the most efficient COS-degrading enzymes and suggesting it as a potential mediator to degrade low concentrations of COS, such as that in the atmosphere.

MATERIALS AND METHODS

More details are given in the Supporting Information.

Purification of COSase. *T. thioparus* strain THI115 (NBRC 105750)²⁶ was harvested by centrifugation, and the cell pellets were disrupted by sonication. COSase was purified from the cell-free extract by column chromatography.

Measurement of COSase Activity. The reaction was started by the addition of 200 μL of the enzyme into a vial (4.9 mL) containing COS and incubated at 30 $^{\circ}\text{C}$ at a static condition. COS and H_2S in the headspace gas was measured by a gas chromatograph equipped with a flame photometric detector (FPD-GC, GC-14B, Shimadzu, Kyoto, Japan). H_2S in the reaction mixture was measured by a colorimetric method.⁴⁸ The amounts of COS in the solution and H_2S in the headspace gas or the solution were estimated based on the solubility of these compounds.^{49–51} COSase activity is expressed as micromoles of H_2S produced per milligram of protein per minute. Also, the TONs are calculated by dimer.

Degradation of Ambient Level COS by Whole Cells. Cells of *T. thioparus* strain THI115 (0.15 g as wet weight) were washed three times and resuspended in a basal salt mTC medium. The resultant cell suspension corresponding to 10 mL-equivalent of culture was filtered with glass fiber filter (GF-75, Advantec Toyo Kaisha, Tokyo, Japan) and then placed on three pieces of wet glass microfiber filters (GF/C circle 90 mm o.d., Whatman, Kent, UK) in 4 mL of mTC medium on the bottom of a Petri dish (9.3 cm i.d.). The dish was placed in a 5 L gas-sampling bag (aluminized polyethylene bag, GL Sciences, Tokyo, Japan) and then exposed to $\sim 3 \text{ L}$ of air. A 300 mL air sample was taken from the bag, loaded onto a pre-cryo column under liquid oxygen, and then introduced to a FPD-GC, as described previously.⁴⁴

Measurement of COSase Activity at Ambient Mixing Ratio of COS. The gas-sampling bag was used for this experiment as described above except N_2 was used instead of air, and pure COS was introduced to make up the final mixing ratio to $\sim 500 \text{ pptv}$. Ten micrograms of COSase in 10 mL of 50 mM Tris-HCl, pH 8.5, was injected onto a glass dish (8.5 cm i.d.) placed in the bag with a syringe through a butyl rubber stopper fitted to the bag. COS was measured by FPD-GC after cryophilic concentration as described above.

Measurement of CO_2 Hydration Activity. The CA activity was measured using stopped-flow spectrophotometry (SX-20, Applied Photophysics, Surrey, UK).⁵² Enzyme solution contained 50 mM Hepes, pH 7.5 as buffer and 0.2 mM phenol red as indicator, and 200 mM Na_2SO_4 to maintain the ionic strength. The enzyme solution and CO_2 -saturated water were mixed 1:1 at 25 $^{\circ}\text{C}$, and the absorbance at 557 nm was measured. CO_2 hydration activity is expressed as μmol of CO_2 hydrated per mg of protein per minute. Also, the TONs are calculated by dimer.

Measurement of CS_2 Hydrolysis Activity. The activity was estimated according to the procedure employed to measurement of COSase activity, except that CS_2 gas (10,200 ppmv in N_2 as a balanced gas, Nissan Tanaka, Saitama, Japan) was used instead of COS. The initial CS_2 concentration in solution was estimated to be 460 μM based on the solubility of 0.047 M atm^{-1} at 30 $^{\circ}\text{C}$.⁵³ After a 20-min incubation, the amount of COS and H_2S in a headspace gas was measured by FPD-GC.

Expression and Purification of Recombinant COSase. The COSase gene was screened from the genomic library and subcloned into a GST fusion protein expression vector. COSase was expressed in *E. coli* and purified by affinity chromatography. The nucleotide sequence data for COSase gene has been submitted to the DDBJ database and will appear in the DDBJ, EMBL, and GenBank nucleotide sequence databases with the accession no. AB583934.

Crystallization and Data Collection. Crystals of COSase were grown at 20 $^{\circ}\text{C}$ using the hanging-drop vapor diffusion method by

mixing 1.2 μL of protein solution (6 $\text{mg}\cdot\text{mL}^{-1}$) with 1.2 μL of reservoir solution (1.2 M $(\text{NH}_4)_2\text{SO}_4$, 0.2 M NaCl, 30% glycerol, 0.1 M Tris-HCl, pH 8.5). Crystals of COSase with SCN^- were obtained by addition of 0.01 M NaSCN to the crystallization drop containing native crystals.

X-ray diffraction data were collected at 95 K using an ADSC/CCD detector system (ADSC Quantum 315r and Quantum 4R) on the BL-5A and BL-6A beamlines at the Photon Factory (Tsukuba, Japan). Diffraction data were processed using the program HKL2000.⁵⁴ Data collection statistics are summarized in Table S2.

Structure Determination and Refinement. The structures of COSase and the COSase/thiocyanate complex were solved by a molecular replacement method with the program Molrep⁵⁵ using the partial structures of β -CA from *Myc. tuberculosis* (PDB code 1YLK, residues 23–99) and the native COSase as a search model, respectively. After a rigid-body refinement using REFMAC,⁵⁶ the model was improved by rebuilding in COOT⁵⁷ and refining in SHELXL.⁵⁸ To avoid over fitting of the diffraction data, a free R-factor was monitored by setting aside 5% of the reflections as a test set.⁵⁹ Finally, the structures were refined to $R_{\text{work}}/R_{\text{free}} = 0.135/0.170$ and $0.156/0.204$ for COSase and COSase/thiocyanate, respectively (Table S2). The atomic coordinates and structure factors for COSase and the COSase/thiocyanate complex were deposited in the PDB under the accession codes 3VQJ and 3VRK, respectively.

ASSOCIATED CONTENT

Supporting Information

Details of materials and methods, Tables S1–S3, and Figures S1–S4. This material is available free of charge via the Internet at <http://pubs.acs.org>.

AUTHOR INFORMATION

Corresponding Author

katayama@cc.tuat.ac.jp

Present Addresses

✉T.O.: Research Center for Science and Technology, Tokyo University of Agriculture and Technology, Fuchu, Tokyo 183-8509, Japan

▽M.S.: Department of Planning, Kamitsuga Agriculture Promotion Office, Kanuma, Tochigi 322-0023, Japan

○Y.N.: JST, ERATO, Suematsu Gas Biology Project, Shinjuku, Tokyo 160-8582, Japan

▲H.K.: Department of Life Sciences, Graduate School of Life Sciences, Tohoku University, Sendai, Miyagi 980-8577, Japan

¶A.O.: Taitec Co., Ltd, Koshigaya, Saitama 343-0822, Japan

Notes

The authors declare no competing financial interest.

ACKNOWLEDGMENTS

This work was supported in part by a Grant-in Aid for Scientific Research from the Ministry of Education, Science, Sports and Culture of Japan (KAKENHI B 18310020 (to Y.K.) and KAKENHI C 22550147 (to K.N.)). We are grateful to the beamline assistants at the Photon Factory for data collection at BL-5A and BL-6A.

REFERENCES

- (1) Chin, M.; Davis, D. D. *J. Geophys. Res.: Atmos.* **1995**, *100*, 8993–9005.
- (2) Andreae, M. O.; Crutzen, P. J. *Science* **1997**, *276*, 1052–1058.
- (3) Crutzen, P. J. *Geophys. Res. Lett.* **1976**, *3*, 73–76.
- (4) Baldwin, B.; Pollack, J. B.; Summers, A.; Toon, O. B.; Sagan, C.; Van Camp, W. *Nature* **1976**, *263*, 551–555.
- (5) Turco, R. P.; Whitten, R. C.; Toon, O. B.; Pollack, J. B.; Hamill, P. *Nature* **1980**, *283*, 283–286.

- (6) Solomon, S.; Sanders, R. W.; Garcia, R. R.; Keys, J. G. *Nature* **1993**, *363*, 245–248.
- (7) Brühl, C.; Lelieveld, J.; Crutzen, P. J.; Tost, H. *Atmos. Chem. Phys.* **2012**, *12*, 1239–1253.
- (8) Aydin, M.; Williams, M. B.; Tatum, C.; Saltzman, E. S. *Atmos. Chem. Phys.* **2008**, *8*, 7533–7542.
- (9) Watts, S. F. *Atmos. Environ.* **2000**, *34*, 761–779.
- (10) Kesselmeier, J.; Teusch, N.; Kuhn, U. *J. Geophys. Res.: Atmos.* **1999**, *104*, 11577–11584.
- (11) Saito, M.; Honna, T.; Kanagawa, T.; Katayama, Y. *Microbes Environ.* **2002**, *17*, 32–38.
- (12) Chengelis, C. P.; Neal, R. A. *Biochem. Biophys. Res. Commun.* **1979**, *90*, 993–999.
- (13) Miller, A. G.; Espie, G. S.; Canvin, D. T. *Plant Physiol.* **1989**, *90*, 1221–1231.
- (14) Kesselmeier, J.; Merk, L. *Biogeochemistry* **1993**, *23*, 47–59.
- (15) Protoschill-Krebs, G.; Wilhelm, C.; Kesselmeier, J. *Bot. Acta* **1995**, *108*, 445–448.
- (16) Protoschill-Krebs, G.; Wilhelm, C.; Kesselmeier, J. *Atmos. Environ.* **1996**, *30*, 3151–3156.
- (17) Haritos, V. S.; Dojchinov, G. *Comp. Biochem. Physiol., Part C: Toxicol. Pharmacol.* **2005**, *140*, 139–147.
- (18) Supuran, C. T. *Nat. Rev. Drug Discovery* **2008**, *7*, 168–181.
- (19) Alterio, V.; Di Fiore, A.; D'Ambrosio, K.; Supuran, C. T.; De Simone, G. *Chem. Rev.* **2012**, *112*, 4421–4468.
- (20) Seefeldt, L. C.; Rasche, M. E.; Ensign, S. A. *Biochemistry* **1995**, *34*, 5382–5389.
- (21) Ensign, S. A. *Biochemistry* **1995**, *34*, 5372–5381.
- (22) Lorimer, G. H.; Pierce, J. J. *Biol. Chem.* **1989**, *264*, 2764–2772.
- (23) Smeulders, M. J.; Barends, T. R. M.; Pol, A.; Scherer, A.; Zandvoort, M. H.; Udvarhelyi, A.; Khadem, A. F.; Menzel, A.; Hermans, J.; Shoeman, R. L.; Wessels, H. J. C. T.; van den Heuvel, L. P.; Russ, L.; Schlichting, I.; Jetten, M. S. M.; Op den Camp, H. J. M. *Nature* **2011**, *478*, 412–416.
- (24) Huber, H.; Stetter, K. O. Genus II. *Acidianus* Segerer, Neuner, Kristjansson and Stetter 1986, 561^{VP}. In *Bergey's Manual of Systematic Bacteriology*, 2nd ed.; Garrity, G. M., Boone, D. R., Castenholz, R. W., Eds.; Springer: New York, 2001; Vol. 1, pp 202–204.
- (25) Kelly, D. P.; Wood, A. P.; Stackebrandt, E. Genus II. *Thiobacillus* Beijerinck 1904b, 597^{AL}. In *Bergey's Manual of Systematic Bacteriology*, 2nd ed.; Garrity, G. M., Brenner, D. J., Krieg, N. R., Staley, J. T., Eds.; Springer: New York, 2005; Vol. 2, Part C, pp 764–769.
- (26) Katayama, Y.; Narahara, Y.; Inoue, Y.; Amano, F.; Kanagawa, T.; Kuraishi, H. *J. Biol. Chem.* **1992**, *267*, 9170–9175.
- (27) Fahey, J. W.; Zalcman, A. T.; Talalay, P. *Phytochemistry* **2001**, *56*, 5–51.
- (28) Valdés, M. G.; Díaz-García, M. E. *Crit. Rev. Anal. Chem.* **2004**, *34*, 9–23.
- (29) Katayama, Y.; Hashimoto, K.; Nakayama, H.; Mino, H.; Nojiri, M.; Ono, T.; Nyunoya, H.; Yohda, M.; Takio, K.; Odaka, M. *J. Am. Chem. Soc.* **2006**, *128*, 728–729.
- (30) Katayama, Y.; Matsushita, Y.; Kaneko, M.; Kondo, M.; Mizuno, T.; Nyunoya, H. *J. Bacteriol.* **1998**, *180*, 2583–2589.
- (31) Arakawa, T.; Kawano, Y.; Kataoka, S.; Katayama, Y.; Kamiya, N.; Yohda, M.; Odaka, M. *J. Mol. Biol.* **2007**, *366*, 1497–1509.
- (32) Kim, S.-J.; Katayama, Y. *Water Res.* **2000**, *34*, 2887–2894.
- (33) Smith, K. S.; Ferry, J. G. *FEMS Microbiol. Rev.* **2000**, *24*, 335–366.
- (34) Rowlett, R. S. *Biochim. Biophys. Acta, Proteins Proteomics* **2010**, *1804*, 362–373.
- (35) Kimber, M. S.; Pai, E. F. *EMBO J.* **2000**, *19*, 1407–1418.
- (36) Holm, L.; Kääriäinen, S.; Rosenström, P.; Schenkel, A. *Bioinformatics* **2008**, *24*, 2780–2781.
- (37) Covarrubias, A. S.; Larsson, A. M.; Högbom, M.; Lindberg, J.; Bergfors, T.; Björkelid, C.; Mowbray, S. L.; Unge, T.; Jones, T. A. *J. Biol. Chem.* **2005**, *280*, 18782–18789.
- (38) Strop, P.; Smith, K. S.; Iverson, T. M.; Ferry, J. G.; Rees, D. C. *J. Biol. Chem.* **2001**, *276*, 10299–10305.
- (39) Covarrubias, A. S.; Bergfors, T.; Jones, T. A.; Högbom, M. *J. Biol. Chem.* **2006**, *281*, 4993–4999.
- (40) De Simone, G.; Supuran, C. T. *J. Inorg. Biochem.* **2012**, *111*, 117–129.
- (41) Minakuchi, T.; Nishimori, I.; Vullo, D.; Scozzafava, A.; Supuran, C. T. *J. Med. Chem.* **2009**, *52*, 2226–2232.
- (42) Smith, K. S.; Ferry, J. G. *J. Bacteriol.* **1999**, *181*, 6247–6253.
- (43) Petřek, M.; Otyepka, M.; Banáš, P.; Košinová, P.; Koča, J.; Damborský, J. *BMC Bioinf.* **2006**, *7*, 316.
- (44) Kato, H.; Saito, M.; Nagahata, Y.; Katayama, Y. *Microbiology* **2008**, *154*, 249–255.
- (45) Smith, K. S.; Jakubzick, C.; Whittam, T. S.; Ferry, J. G. *Proc. Natl. Acad. Sci. U.S.A.* **1999**, *96*, 15184–15189.
- (46) Li, X. S.; Sato, T.; Ooiwa, Y.; Kusumi, A.; Gu, J.-D.; Katayama, Y. *Microb. Ecol.* **2010**, *60*, 96–104.
- (47) Ueno, Y.; Johnson, M. S.; Danielache, S. O.; Eskebjerg, C.; Pandey, A.; Yoshida, N. *Proc. Natl. Acad. Sci. U.S.A.* **2009**, *106*, 14784–14789.
- (48) Chae, Y. M.; Tabatabai, M. A. *Anal. Lett.* **1983**, *16*, 1197–1206.
- (49) Wilhelm, E.; Battino, R.; Wilcock, R. J. *Chem. Rev.* **1977**, *77*, 219–262.
- (50) De Bruyn, W. J.; Swartz, E.; Hu, J. H.; Shorter, J. A.; Davidovits, P.; Worsnop, D. R.; Zahniser, M. S.; Kolb, C. E. *J. Geophys. Res.: Atmos.* **1995**, *100*, 7245–7251.
- (51) Dean, J. A. *Electrolytes, Electromotive Force, and Chemical Equilibrium: Lange's Handbook of Chemistry*, 15th ed.; McGraw-Hill: New York, 1999; pp 8.1–8.169.
- (52) Khalifah, R. G. *J. Biol. Chem.* **1971**, *246*, 2561–2573.
- (53) Staudinger, J.; Roberts, P. V. *Chemosphere* **2001**, *44*, 561–576.
- (54) Otwinowski, Z.; Minor, W. *Methods Enzymol.* **1997**, *276*, 307–326.
- (55) Vagin, A.; Teplyakov, A. *J. Appl. Crystallogr.* **1997**, *30*, 1022–1025.
- (56) Murshudov, G. N.; Vagin, A. A.; Dodson, E. J. *Acta Crystallogr., Sect. D: Biol. Crystallogr.* **1997**, *53*, 240–255.
- (57) Emsley, P.; Cowtan, K. *Acta Crystallogr., Sect. D: Biol. Crystallogr.* **2004**, *60*, 2126–2132.
- (58) Sheldrick, G. M. *Acta Crystallogr., Sect. A: Found. Crystallogr.* **2008**, *64*, 112–122.
- (59) Brünger, A. T. *Nature* **1992**, *355*, 472–475.
- (60) Tamura, K.; Peterson, D.; Peterson, N.; Stecher, G.; Nei, M.; Kumar, S. *Mol. Biol. Evol.* **2011**, *28*, 2731–2739.